

A combined spin trapping/EPR/mass spectrometry approach to study the formation of a cyclic peroxide by dienolic precursor autoxidation†

Mathilde Triquigneaux,^a Laurence Charles,^a Christiane André-Barrès^b and Béatrice Tuccio^{*a}

Received 19th October 2009, Accepted 17th December 2009

First published as an Advance Article on the web 21st January 2010

DOI: 10.1039/b921694d

The spontaneous addition of air oxygen to a dienolic compound, yielding a cyclic peroxide, was followed by spin trapping (ST) combined with EPR spectroscopy and mass spectrometry (MS). Using two different nitrones, the ST/EPR study allowed the detection of the spin adduct of a radical intermediate, and the radical centre in the addend was identified after similar experiments performed with two different ¹³C-labelled analogues of the substrate. The media were also submitted to electrospray ionisation, in both positive and negative modes, for structural characterisation of the spin adducts by tandem mass spectrometry. This allowed the structure of the hydroxylamine derivatives of the nitroxides formed to be identified. Following these results, a mechanism pathway was proposed for this autoxidation.

Introduction

G-factors are natural compounds acting as phytohormones, growth regulators and intervening in plant defence in *Eucalyptus grandis* and other *Myrtaceae*.¹ Several natural or synthetic G-factors showed interesting antiparasitic activities related to the presence of a peroxide bridge,² also found in a large series of other antimalarial compounds (e.g. artemisinin, BO7, artefene or trioxaquinones).³ Since the cyclic peroxide **2** could be formed after oxygen uptake from air by the dienolic system **1a** (which is in equilibrium with a dienone form), this autoxidation was used as the key step in the synthesis of various G-factors (see Scheme 1a).⁴ The reaction is quantitative, selective, performed at room temperature in very mild conditions, even in the solid state, producing no waste and maximising atom economy. It could thus constitute an environmentally benign green chemical process to synthesise cyclic peroxides. Since then, efforts have been made to elucidate the mechanism of this intriguing reaction.^{4,5} It proceeds in the dark by adding oxygen from air, without any activation or sensitiser. A photo- or a base-catalysed oxidation, the intervention of singlet dioxygen or an electron transfer between O₂ and the substrate are all processes that have been discarded based on various experiments. On the other hand, this peroxidation was inhibited by a catalytic amount of the radical scavenger *tert*-butanethiol, which led us to examine the possibility that **1a** could behave as a radicaloid in a reaction with triplet oxygen avoiding the spin barrier. Although such a mechanism is unusual, several other “forbidden” additions of triplet oxygen to singlet substrates have been reported.⁶ A preliminary study of the autoxidation of **1a** into **2** was performed using the spin-trapping (ST)/electron paramag-

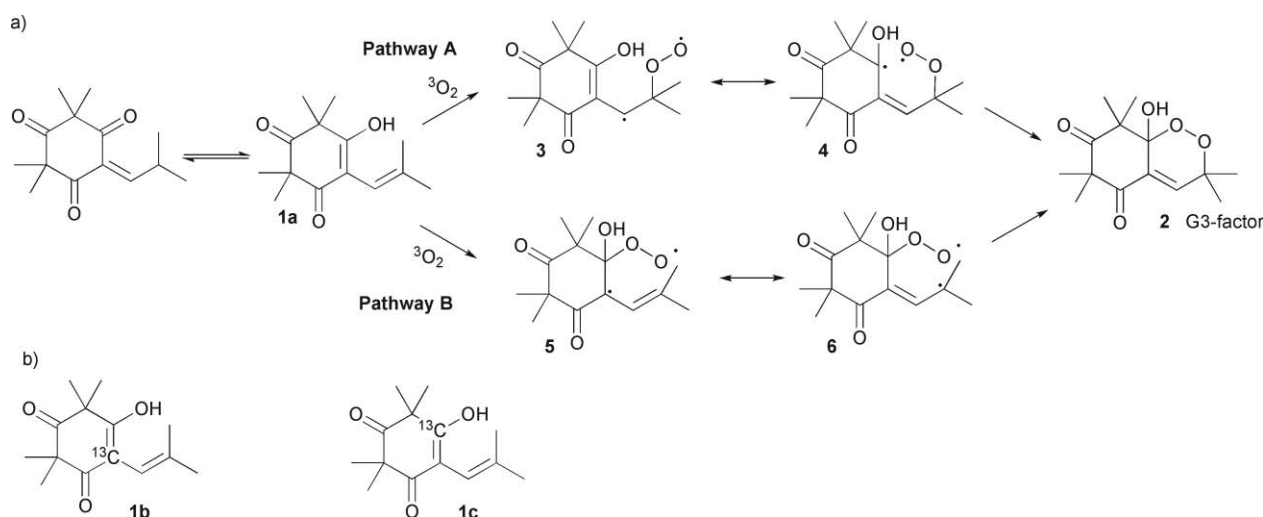
netic resonance (EPR) methodology.⁷ The ST technique relies on the fast addition of a transient radical to a diamagnetic spin trap (usually a nitron or a nitroso compound) to yield a longer-lived paramagnetic spin adduct (a nitroxide) that can be detected by conventional EPR spectroscopy (see Scheme 2). Analysing the EPR spectrum obtained gives information about the addend structure. Using 2-methyl-2-nitrosopropane (MNP) and diethyl (2-methyl-1-oxido-3,4-dihydro-2*H*-pyrrol-2-yl) phosphonate (DEPMPO) as spin traps, carbon-centred radical intermediates formed during **1a** autoxidation were detected. However, we did not gain much information about the structure of the radical trapped using the sole EPR spectroscopy, and both structures **3** and **5**, corresponding to two different reaction pathways, were then postulated for the intermediate initially formed (see Scheme 1a).

Recently, we described several applications of ST coupled with mass spectrometry (MS) for free radical characterisation.⁸ The feasibility of using tandem mass spectrometry (MS/MS) for direct identification of nitroxide spin adducts electrosprayed from complex mixtures, without prior chromatographic separation, was thus demonstrated. This method also brought valuable information about diamagnetic products derived from the nitroxide initially formed. The purpose of this work was to proceed with the study of the mechanism of ³O₂ addition on **1a** using a combined ST/EPR/MS approach. With the help of this powerful tool, our aim was *i*) to confirm with non-cyclic nitrones the ST/EPR results previously obtained with MNP and DEPMPO, *ii*) to discriminate the different conceivable reaction pathways and *iii*) to elucidate the structures of various reaction intermediates. Therefore, two nitrones, the commercially available 4-[(*E*)-[*tert*-butyl(oxido)imino]methyl]pyridine 1-oxide (POBN), and the ³¹P-labelled trinitrone diethyl {1-[(*Z*)-(3,5-bis[(*E*)-[[1 (diethoxyphosphoryl)-1-methylethyl](oxido)imino]methyl]-benzylidene)(oxido)amino]-1-methylethyl]phosphonate (TN), were employed to trap radical intermediates formed during the autoxidation of three dienolic precursors, *i.e.* **1a** and its ¹³C-labelled analogues **1b** and **1c** (see Schemes 1 and 2). Then, both conventional X-band EPR detection and electrospray ionisation mass spectrometry (ESI-MS) were employed to

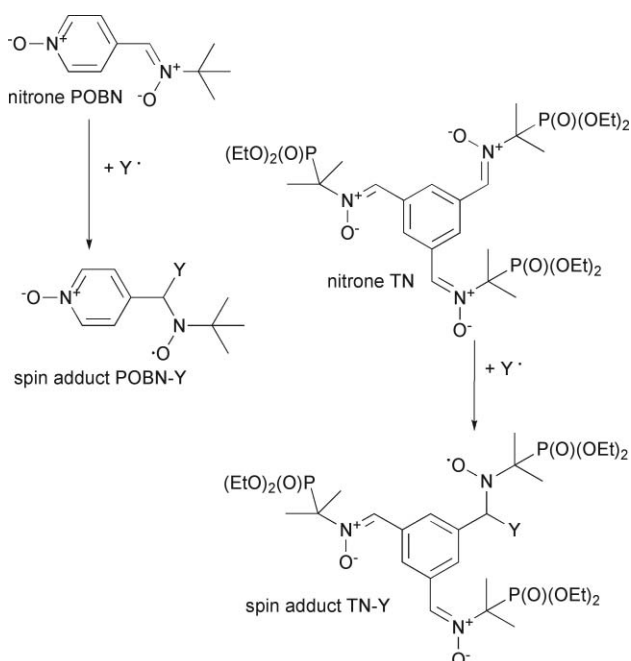
^aUniversités Aix-Marseille I, II & III–CNRS, UMR 6264: Laboratoire Chimie Provence, Spectrométries Appliquées à la Chimie Structurale, 13397 Marseille Cedex 20, France; Fax: (+33) 491282897; Tel: (+33) 491288743. E-mail: beatrice.tuccio-lauricella@univ-provence.fr

^bUniversité Paul Sabatier–CNRS, UMR 5068: Synthèse et Physico-Chimie des Molécules d'Intérêt Biologique, 31062 Toulouse Cedex, France

† Electronic supplementary information (ESI) available: ESI-MS/MS of **1a** and of **18**, in positive and negative modes. See DOI: 10.1039/b921694d



Scheme 1 a) Formation of the G3-factor **2** by spontaneous addition of dioxygen on the dienolic precursor **1a** according to two possible pathways **A** and **B**, and structures of the biradical intermediates **3–6** postulated for this reaction; b) formulae of the ^{13}C -labelled analogues of **1a** considered in this study.



Scheme 2 Spin trapping of a radical Y^\bullet using the nitrones POBN or TN and structures of the nitroxide spin adducts formed.

detect and characterise the spin adducts formed as well as their derivatives.

Experimental

Materials

POBN was purchased from Sigma-Aldrich (St. Louis, MO). Methanol (SDS, Peypin, France), acetonitrile and benzene (Sigma-Aldrich) were of the highest grade of purity commercially available and used as received. Poly(ethylene glycol) with M_n 400 g mol^{-1} (Sigma-Aldrich) was used as an internal standard for accurate mass measurements. TN was synthesised and purified as described elsewhere.⁹ The dienolic precursors **1a**, **1b** and **1c** were

prepared according to procedures described previously and stored under argon to avoid autoxidation.^{5b} The cyclic peroxide **2** was obtained after air oxidation of **1a**.⁴

Spin trapping

Spin adducts were produced by mixing the dienolic precursor (**1a–1c**, 0.2 mol dm^{-3}) and the spin trap (0.2 mol dm^{-3} POBN or 0.1 mol dm^{-3} TN) in oxygenated benzene. The system was allowed to react for 1 h, and the sample was deoxygenated by nitrogen bubbling before EPR analysis. For each experiment, 300 μL of reaction medium was prepared. An aliquot (*ca.* 30 μL) was transferred into a glass pipette closed with a septum for EPR analysis, while 50 μL was diluted in methanol (1/10, vol/vol) for MS analysis.

EPR spectroscopy

EPR assays were carried out at room temperature by using a Bruker EMX spectrometer operating at X-band with 100 kHz modulation frequency, and equipped with an NMR gaussmeter for magnetic field calibration. The instrument settings were as follows: non-saturating microwave power, 20 mW; modulation amplitude, 0.15 mT; receiver gain, 1×10^6 ; time constant, 1.28 ms; scan time, 120 s; scan width, 10–20 mT. Hyperfine coupling constant (hfcc) and g -tensor values were obtained after computer simulation of the EPR spectra using the software elaborated by Duling.¹⁰

Mass spectrometry

High-resolution MS and MS/MS experiments were performed with a QStar Elite mass spectrometer (Applied Biosystems SCIEX, Concord, ON, Canada) equipped with an electrospray ionisation source. In the positive ion mode, the capillary voltage was set at 5500 V and the cone voltage at 80 V. For experiments performed in the negative ion mode, the capillary voltage was -4500 V and the cone voltage was -70 V. In this hybrid instrument, ions were measured using an orthogonal acceleration time-of-flight (oa-TOF) mass analyser. A quadrupole was used for selection

of precursor ions to be further submitted to collision induced dissociation (CID) in MS/MS experiments. In MS, accurate mass measurements were performed using two reference ions from a poly(ethylene glycol) internal standard, according to a procedure described elsewhere.¹¹ The precursor ion was used as the reference for accurate measurements of product ion m/z ratio in MS/MS spectra. In the instrument, air was used as the nebulising gas (10 psi) whereas nitrogen was used as the curtain gas (20 psi) as well as the collision gas. Collision energy was set according to the experiments. Instrument control, data acquisition and data processing of all experiments were achieved using Analyst software (QS 2.0) provided by Applied Biosystems. Sample solutions were introduced in the ionisation source at a $5 \mu\text{L min}^{-1}$ flow rate using a syringe pump.

Results and discussion

ST/EPR study

Two linear aldonitrone, POBN and TN, were used to trap free radicals produced during **1a–1c** autoxidation. In order to simplify the notation, the nitroxide formed by trapping a radical Y^\bullet by POBN or TN will be denoted POBN- Y or TN- Y , respectively (see Scheme 2). A standard EPR spectrum of a POBN- Y nitroxide shows six lines due to hyperfine couplings of the unpaired electron with the nitrogen and the β -hydrogen nuclei. In the case of TN- Y , this sextuplet is split by a large extra coupling with the phosphorus nucleus, resulting in a twelve line EPR spectrum. The hyperfine coupling constants (hfccs) with the nitrogen, the β -hydrogen and the β -phosphorus nuclei will be denoted a_N , a_H and a_P , respectively.

Preparing a benzene solution containing **1a**, POBN and O_2 allowed us to record the spectrum given in Fig. 1a, which revealed the presence of two nitroxides. The major species EPR signal exhibited six lines ($g = 2.00619$, $a_N = 1.64 \text{ mT}$ and $a_H = 0.16 \text{ mT}$, 82%) and could be assigned to a carbon-centred radical adduct denoted POBN-C, on the basis of the results previously obtained with DEPMPO⁷ and by comparison with literature data.¹² The minor signal ($g = 2.00660$, $a_N = 1.36 \text{ mT}$ and $a_{\text{HP}} = 1 \text{ mT}$, 18%) showed a much lower a_H value, often characteristic of an oxygen-centred radical adduct.¹³ Complementary experiments were performed to establish whether this adduct was formed after trapping a peroxy radical RO_2^\bullet , as suggested in the study realised with DEPMPO,⁷ or an alkoxyl radical RO^\bullet , formed after homolytic ring opening in the final cyclic peroxide.⁵ POBN (0.2 mol dm^{-3}) and **2** (0.2 mol dm^{-3}) were dissolved in acetonitrile (**2** being poorly soluble in benzene) and the medium was passed through a metallic needle in order to add metal traces. EPR analysis of the medium revealed the presence of a single nitroxide, with $g = 2.00660$, $a_N = 1.36 \text{ mT}$ and $a_{\text{HP}} \leq 0.12 \text{ mT}$. Though the lines were too broad to allow an accurate determination of a_H , these EPR parameters resemble very much that of the oxygen-centred radical adduct resulting from the reaction between **1a** and O_2 in the presence of POBN. Therefore, we can reasonably assign the minor species detected in the former experiments to POBN-OR, a by-product formed after trapping an alkoxyl radical originating from a O–O bond break in **2**, rather than to a peroxy radical adduct.

The same kind of experiment was then conducted with the spin trap TN, which presents two main advantages when compared

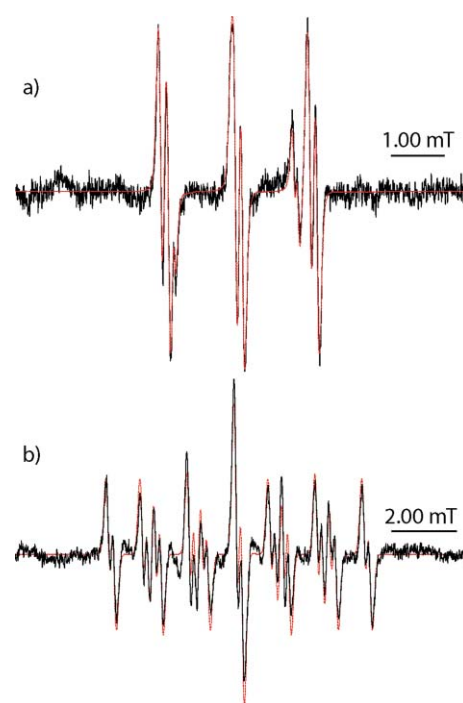


Fig. 1 Experimental EPR signals (black full lines) obtained in deoxygenated benzene after 1 h of reaction between molecular oxygen and (a) **1a** (0.2 mol dm^{-3}) in the presence of POBN (0.2 mol dm^{-3}), and (b) **1b** (0.2 mol dm^{-3}) in the presence of TN (0.1 mol dm^{-3}). Their superimposed simulations (red dotted lines) led to the following parameters: signal (a) 82% POBN-C ($g = 2.00619$, $a_N = 1.64 \text{ mT}$ and $a_H = 0.16 \text{ mT}$) and 18% POBN-OR ($g = 2.00660$, $a_N = 1.36 \text{ mT}$ and $a_{\text{HP}} = 0.1 \text{ mT}$); signal (b) 100% TN- ^{13}C ($g = 2.00624$, $a_N = 1.55 \text{ mT}$, $a_H = 0.19 \text{ mT}$, $a_P = 4.26 \text{ mT}$ and $a_{\text{OC}} = 1.14 \text{ mT}$).

to POBN. First, the EPR spectra of its various spin adducts usually provide more information about the addend, because the strong hfcc a_P is very sensitive to the nature of the radical trapped. In addition, the presence of three nitrone functions on TN greatly enhances the radical trapping rates, without leading to the formation of a significant amount of di- or tri-nitroxide when TN concentration is higher than 0.02 mol dm^{-3} .⁹ Mixing **1a** (0.2 mol dm^{-3}) and TN (0.1 mol dm^{-3}) in oxygenated benzene gave rise to an intense twelve line EPR spectrum, showing the presence of a single mono-nitroxide. Its analysis resulted in the following parameters: $g = 2.00624$, $a_N = 1.55 \text{ mT}$, $a_H = 0.19 \text{ mT}$ and $a_P = 4.26 \text{ mT}$. This nitroxide was identified as the TN spin adduct of a radical centred on a sterically hindered carbon, *i.e.* TN-C, by comparison with the literature data.^{9,14} It is worth mentioning that the nitroxide TN-OR was never observed in these experiments, and two hypotheses were envisaged to explain this result. The first one relates to kinetic criteria. Just after the initial addition of O_2 to **1a**, two competitive reactions should be considered: the ring closure, leading to **2**, and the spin trapping of a radical intermediate. The formation of RO^\bullet , originating from the cyclic peroxide bridge break, necessitates the presence in the medium of a significant amount of **2**. With the nitrone POBN, the trapping kinetics were slow enough to allow the generation of RO^\bullet and its subsequent addition to the nitrone, and POBN-OR was detected as a minor by-product. Since the rates of free radical trapping by TN are much higher,^{9,15} the amount of RO^\bullet in the medium could be too low to be

observed by ST/EPR. Note however that no signal was detected when a solution containing TN (0.1 mol dm^{-3}), **2** (0.2 mol dm^{-3}) and metal traces in acetonitrile was analysed by EPR, which goes against this first hypothesis. Alternatively, trace metal impurities eventually present in the medium could form inactive complexes with the phosphonate groups borne on TN, which would hamper the peroxide ring opening reaction. Whatever it may be, these results refute the hypothesis of a peroxy radical trapping.

The experiments performed with both POBN and TN confirm the formation of carbon-centred radical intermediates during **1a** autoxidation and produces further evidence of a radical pathway for this reaction. At this point however, the actual mechanism of this reaction remains ambiguous because the adduct characteristics as indicated by EPR did not reveal much about the exact structure of the species trapped. In particular, the two possible pathways **A** and **B** depicted in Scheme 1 would allow the formation of the intermediate isomers **3–6**. In order to identify the actual radical intermediate, further spin trapping experiments were performed using the ^{13}C -labelled precursors **1b** and **1c**. The EPR spectrum recorded from an oxygenated benzene solution containing **1b** and POBN, revealed the presence of two nitroxides only. The minor species ($g = 2.00660$, $a_{\text{N}} = 1.36 \text{ mT}$ and $a_{\text{H}\beta} = 0.10 \text{ mT}$, 10%) could be clearly identified as the spin adduct POBN-OR, formed after trapping the free radical resulting from the ring opening in the final cyclic peroxide. The predominant EPR signal (90%) showed twelve lines, because of an extra hyperfine coupling with the ^{13}C nucleus in the β -position towards the nitrogen, with the following parameters: $g = 2.00619$, $a_{\text{N}} = 1.64 \text{ mT}$, $a_{\text{H}} = 0.16 \text{ mT}$ and $a_{^{13}\text{C}} = 1.14 \text{ mT}$. These data clearly suggest that the ^{13}C carbon is the radical centre that added to the nitron function during the trapping reaction, and the spin adduct detected was thus denoted POBN- ^{13}C . The same kind of results were obtained with the spin trap TN. Reacting dioxygen on **1b** in the presence of TN in benzene gave rise to the intense EPR signal shown in Fig. 1b. Its analysis revealed the presence of a single nitroxide which, on the basis of its EPR parameters ($g = 2.00624$, $a_{\text{N}} = 1.55 \text{ mT}$, $a_{\text{H}} = 0.19 \text{ mT}$, $a_{\text{P}} = 4.26 \text{ mT}$ and $a_{^{13}\text{C}} = 1.14 \text{ mT}$) could be identified as TN- ^{13}C , the spin adduct obtained after trapping a radical intermediate centred on the ^{13}C atom. All these results clearly point to the fact that the spin adducts detected, *i.e.* POBN- ^{13}C and TN- ^{13}C , came from the initial formation of the biradical **5** only. In both adducts, the $a_{^{13}\text{C}}$ values were higher than those frequently observed for a splitting due to a ^{13}C in the β -position towards a nitroxide nitrogen. Since this hyperfine coupling depends on the dihedral angle between the planes $\text{C}_{\beta}\text{C}_{\alpha}\text{N}$ and $\text{C}_{\alpha}\text{Np}_{\text{z}}$, substituents may greatly modify $a_{^{13}\text{C}}$, as shown for instance by Rockenbauer *et al.*¹⁶ In the case of POBN- ^{13}C and TN- ^{13}C , the steric hindrance due to the bulky radical captured by the two PBN-type nitrones should yield a particular conformation in which the C_{α} - ^{13}C bond is almost orthogonal to the nitroxide plane $\text{C}_{\alpha}\text{NO}$, resulting in the high $a_{^{13}\text{C}}$ values determined.

The same kind of experiment was also performed with the ^{13}C -analogue **1c** with both POBN and TN. The spin adducts thus detected showed EPR spectra identical to those obtained with the non-labelled precursor **1a**, indicating that the carbon-centred radical trapped did not correspond to the intermediate **4**. In all these experiments, we never observed any spin adduct derived from **6**, regardless of the nitron or of the dienolic precursor used. Though the mesomeric intermediates **5** and **6** both present an

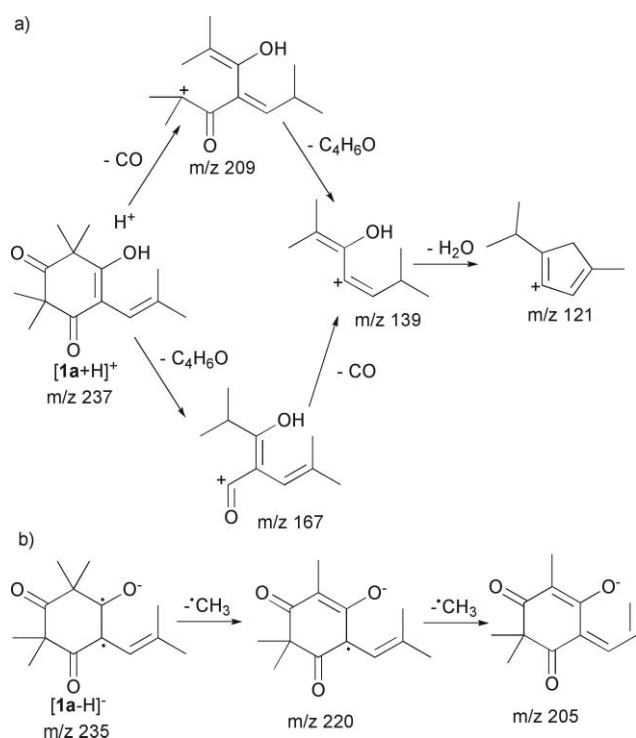
unpaired electron on a tertiary carbon, the cyclisation reaction in the resonance form **6** seems to be a much faster process than the trapping reaction.

This ST/EPR study is fully consistent with the pathway **B** for this autoxidation reaction, but it does not necessarily imply that the pathway **A** did not occur simultaneously. Neither **3** nor **4** was ever observed in these ST/EPR experiments, but it could not be concluded that these alternative intermediates were not created during the endoperoxidation reaction without considering the kinetic aspects. Actually, if the ring closure yielding **2** in pathway **A** is much faster than the trapping reactions, no spin adduct derived from either **3** or **4** would ever be detected. Note also that, in a previous work concerning the search for new antimalarial cyclic peroxides related to G-factor series, cyclic ether alcohols and hydroperoxides were obtained besides cyclic peroxides after autoxidation of the dienol intermediate step.¹⁷ The formation of these unexpected compounds were explained by evolution of the postulated biradical intermediate **3** following pathway **A**. Pursuing this hypothesis, a mechanism was proposed in which biradical species participate but in this special case could evolve differently from the sole formation of cyclic peroxides as described in previous reports.¹⁷ Taking these results into account, the present ST/EPR study only proved that the pathway **B** occurred in our experimental conditions, but does not allow pathway **A** to be discarded as an alternative or even as a main process.

Mass spectrometry study

Compounds generated during the reaction of the dienol- O_2 biradical with POBN or TN could not be precisely defined by EPR spectroscopy, which focuses on the detection of the sole paramagnetic function, and does not provide information about the global structure. More particularly, a predominant mono-radical carbon-centred spin adduct was detected, with no indication about the rearrangement of the oxygen part in the bi-radical intermediate. Therefore, the ST/EPR/MS approach⁸ was used to characterise the spin adduct structures.

Since no MS study of **1a** has ever been described, this compound was first analysed by ESI-MS/MS, to establish a referenced fragmentation behaviour to be further used in the structural characterisation of spin adducts. The positive mode ESI-MS spectrum showed a peak at m/z 237.1 which could be assigned to the protonated dienol, $[\mathbf{1a} + \text{H}]^+$. Upon CID, this precursor ion gave rise to a main product ion at m/z 139.1 as well as three other minor products at m/z 209.1, m/z 167.1 and m/z 121.1 (see Electronic Supplementary Information, Fig. S1). Accurate mass measurements allowed us to propose the fragmentation pathways depicted in Scheme 3a. Elimination of a CO molecule from $[\mathbf{1a} + \text{H}]^+$ would produce m/z 209.1524 ($\text{C}_{13}\text{H}_{21}\text{O}_2^+$, +5.7 ppm) from which the loss of a 2-methylprop-1-en-1-one ($\text{C}_4\text{H}_6\text{O}$) would give rise to m/z 139.1117 ($\text{C}_9\text{H}_{15}\text{O}^+$, -0.3 ppm). Alternatively, this m/z 139.1 product ion could be formed after the precursor ion has first eliminated the $\text{C}_4\text{H}_6\text{O}$ moiety to yield m/z 167.1062 ($\text{C}_{10}\text{H}_{15}\text{O}_2^+$, +2.7 ppm), then the neutral CO. Finally, dehydration of m/z 139.1 would produce m/z 121.1012 ($\text{C}_9\text{H}_{13}^+$, +0.2 ppm) *via* a cyclisation mechanism. In the negative ion mode, the deprotonated dienol could be observed at m/z 235.1 in the ESI-MS spectrum. CID experiments revealed that $[\mathbf{1a} - \text{H}]^-$ dissociates *via* a main pathway, consisting of two successive eliminations of a methyl radical to



Scheme 3 Fragmentation pattern of (a) $[1a + H]^+$ and (b) $[1a - H]^-$.

respectively produce m/z 220.1110 ($C_{13}H_{16}O_3^+$, -2.7 ppm) and m/z 205.0868 ($C_{12}H_{13}O_3^+$, $+0.8$ ppm), as illustrated in Scheme 3b. The first $\cdot CH_3$ loss appears as an exception to the even-electron rule¹⁸ but could be explained by the radicaloid character of **1a** in its deprotonated form, as illustrated in Scheme 3b.

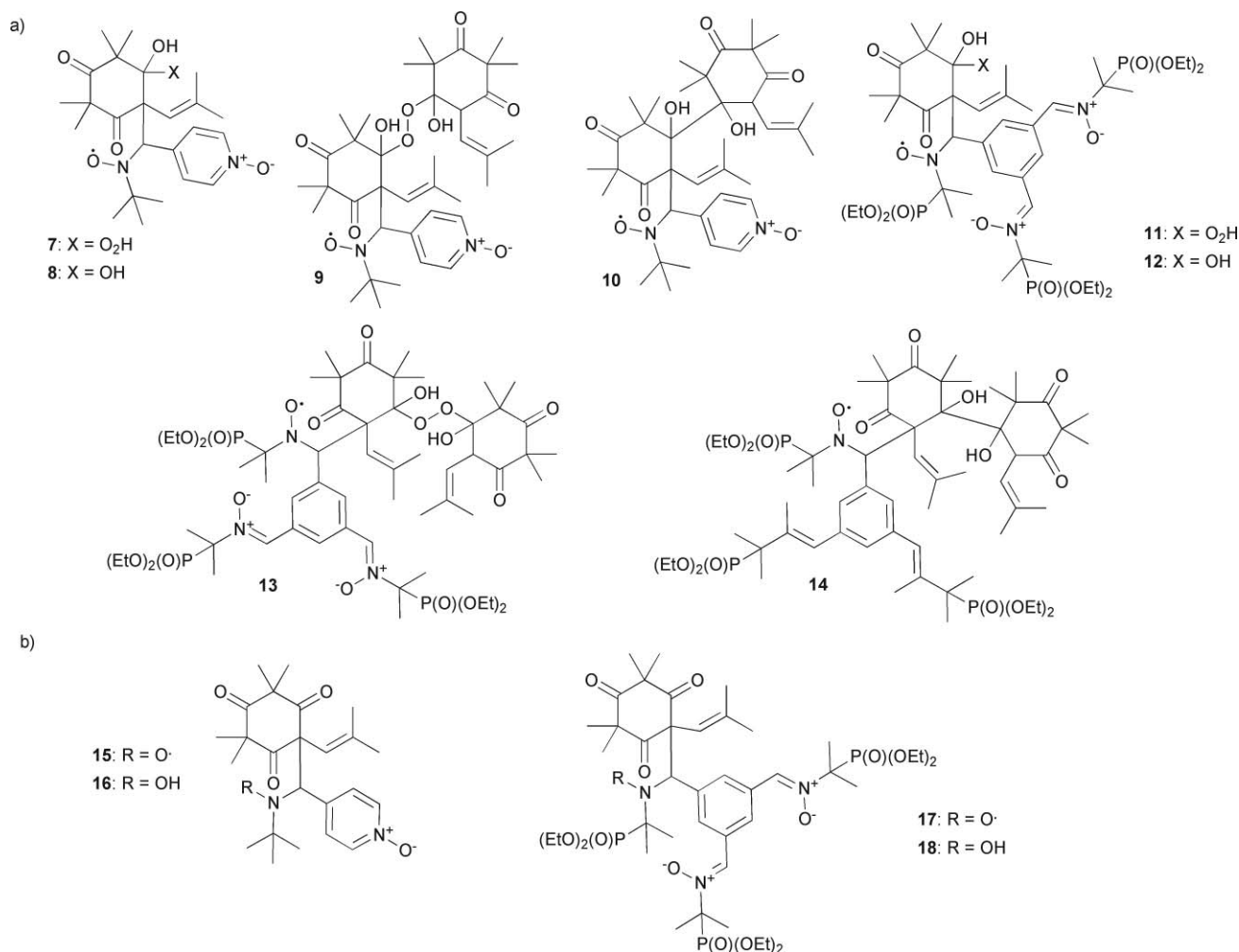
The reaction medium in which the nitroxide adduct POBN-C was produced and detected in EPR was then submitted to electrospray ionisation after diluting the organic solution in methanol. The so-obtained ESI-mass spectrum was scrutinised for signals diagnostic of the different protonated spin adducts that could be envisaged to be formed during spin trapping of the intermediate **5**. Indeed, various rearrangements of **5**, prior or after spin trapping, can be assumed. A first derivative **7** could be formed after reduction of the peroxy radical of the nitroxide spin adduct into hydroperoxide to generate a protonated compound at m/z 464.3 in ESI-MS. An alcohol group could also be formed upon evolution of the peroxy part, generating the geminated-diol compound **8** which should be detected as a protonated molecule at m/z 448.3. Finally, bimolecular rearrangements have also been envisaged, leading to molecules **9** and **10** that would be respectively detected at m/z 699.4 and at m/z 667.4 in their protonated forms. The structure of these proposed derivatives are detailed in Scheme 4. Neither the intact POBN/**5** adduct nor any of the proposed derivatives could be detected during mass spectrometric experiments. Alternatively, the carbon position related to both hydroxyl group and peroxy radical in **5** could rearrange in a carbonyl group, giving rise to a protonated nitroxide expected at m/z 430.3 in mass spectrometry. Actually, the positive mode ESI mass spectrum showed a peak at m/z 431.3, which was assigned to the protonated hydroxylamine, $[16 + H]^+$, presumably derived from the spin adduct **15** (see Scheme 4). This result was further supported in negative mode MS experiments which showed a

signal at m/z 429.2, assigned to the deprotonated hydroxylamine $[16 - H]^-$.

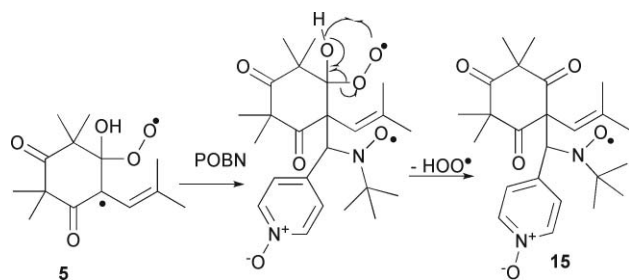
A similar approach was followed to scrutinise the ESI mass spectra obtained in the case of the spin adduct TN-C. The same structural assumptions were proposed for derivatives of the spin adduct involving TN and **5**, that is, compounds **11–14** resulting from the addition of a H^\bullet on the peroxy radical moiety (m/z 1011.4), the rearrangement in diol (m/z 995.4) and bimolecular association (m/z 1247.4 and m/z 1279.4). Again, none of these species could be mass detected and, as in the case of POBN, a peak at m/z 978.4 in positive mode ESI-MS and a signal at m/z 976.4 in the negative ion mode suggested the detection of the hydroxylamine **18** diagnostic of the formation of **17** during spin trapping experiments (see Scheme 4). These assignments were mainly based on m/z values measured in the MS spectra and low abundance of the targeted ions did not allow good quality accurate mass measurements.¹¹ MS/MS experiments were thus required to validate the structure proposed in Scheme 4.

As can be seen in Fig. 2a, CID of $[16 + H]^+$ at m/z 431.3 produced two main fragment ions at m/z 195.1 and m/z 139.1. Assuming a $C_{24}H_{35}N_2O_5^+$ composition for the precursor ion to calibrate this MS/MS spectrum, accurate mass measurement indicates that m/z 195.1124 ($C_{10}H_{15}N_2O_2^+$, $+1.7$ ppm) would correspond to the protonated POBN molecule, arising from the elimination of the **1a** neutral from the precursor ion. The m/z 139.1 product ion (m/z 139.0480, $C_6H_7N_2O_2^+$, $+15.8$ ppm) would thus result from the loss of a 2-methylpropene from m/z 195.1, a typical dissociation reaction observed during CID of protonated POBN. MS/MS experiments performed on the deprotonated hydroxylamine **16** were shown to provide complementary information to data obtained in the positive ion mode. Indeed, the main product ion generated upon CID of $[16 - H]^-$ (Fig. 2b) could be assigned to a deprotonated **1a** molecule (m/z 235.1304, $C_{14}H_{19}O_3^-$, $+15.4$ ppm) formed after the elimination of a POBN neutral from the precursor ion. This assignment was further supported by data obtained at higher collision energy (60 eV, laboratory frame) which showed the typical m/z 220.1 and m/z 205.1 product ions of $[PG3 - H]^-$ (*vide supra*). It could thus be concluded from these MS/MS data that the ionic species observed at m/z 431.1 in the positive mode and at m/z 429.2 in the negative mode were respectively the protonated and the deprotonated form of the hydroxylamine **16**.

A similar approach was followed to validate the structure proposed for the hydroxylamine **18** (see Electronic Supplementary Information, Figure S2). In positive mode, a unique product ion (m/z 742.3089, $C_{30}H_{55}N_3O_{12}P_3^+$, -13.0 ppm) was observed after the dissociation of $[18 + H]^+$, which could be assigned to a protonated TN nitron formed after elimination of a **1a** moiety from the precursor ion. The intense peak measured at m/z 235.1320 ($C_{14}H_{19}O_3^-$, $+8.6$ ppm) in the MS/MS spectrum of $[18 - H]^-$, would arise from the elimination of a TN neutral leading to a deprotonated **1a** molecule. As in the case of **16**, the complementary data obtained while performing MS/MS experiments in both polarity modes allows us to validate the structure proposed for the hydroxylamine **18**. Detection of the hydroxylamine species in mass spectrometry would indicate that the paramagnetic species observed in EPR experiments were **15** and **17**. These nitroxides could result from the trapping of **5** followed by a fast conversion of the peroxy radical moiety into a



Scheme 4 a) Various structures 7–14 hypothesised for the spin adducts POBN-C and TN-C and discarded after ESI-MS experiments and b) structures 15–18 proposed for POBN-C and TN-C spin adducts and for their hydroxylamine derivatives based on ESI-MS results.



Scheme 5 Mechanism assumed for the formation of 15.

ketone function. This release of HO₂^{*} could not occur in **5** before the spin trapping process. In this case, this process would also take place in the absence of spin trap, which contradicts the quantitative formation of the cyclic peroxide **2** from **1** autoxidation. Following all these results, the mechanism assumed for the formation of the spin adducts detected is illustrated by Scheme 5 in the case of POBN-C.

Conclusions

This work clearly demonstrates that the cyclic peroxide synthesis by autoxidation of the dienolic precursor **1a** corresponds to a radical process, thereby confirming the main result obtained in our preliminary ST/EPR study.⁷ Whatever the nitron, a single mono-radical nitroxide, *i.e.* a carbon-centred radical spin adduct, was EPR-detected in the ST experiments performed, and the use of ¹³C-labelled precursors allowed us to identify the radical centre in the addend. The ST/MS technique, used without preliminary chromatographic purification, provided a powerful tool, complementary to EPR, for the identification of the radical intermediates. In particular, the structure of the spin adducts POBN-C and TN-C could be elucidated after MS/MS experiments. All the EPR and MS results obtained led us to conclude that the conversion of the dienolic precursor **1a** into the G-factor **2** could follow the pathway **B** (see Scheme 1) in the experimental conditions considered here, though pathway **A** could not be dismissed at present. Finally, this combined ST/EPR/MS approach was demonstrated to be a powerful tool for mechanism studies in radical chemistry.

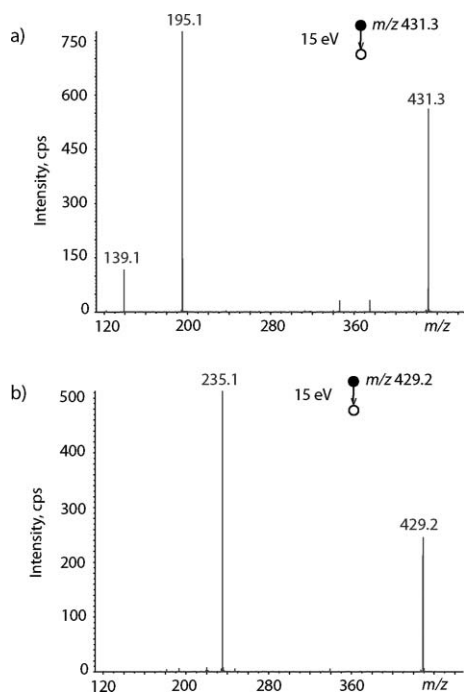


Fig. 2 ESI-MS/MS of a) $[16 + H]^+$ at 15 eV and b) $[16 - H]^-$ at 15 eV.

Acknowledgements

L. Charles acknowledges support from Spectropole, the Analytical Facility of Aix-Marseille University, by allowing a special access to the instruments purchased with European Funding (FEDER OBJ2142-3341).

Notes and references

- 1 E. Ghisalberti, *Phytochemistry*, 1996, **41**, 7.
- 2 (a) F. Najjar, M. Baltas, L. Gorrichon, Y. Moreno, H. Vial, T. Tzedakis and C. André-Barrès, *Eur. J. Org. Chem.*, 2003, 3335; (b) F. Najjar, L. Gorrichon, M. Baltas, H. Vial, T. Tzedakis and C. André-Barrès, *Bioorg. Med. Chem. Lett.*, 2004, **14**, 1433; (c) F. Najjar, L. Gorrichon, M. Baltas, H. Vial and C. André-Barrès, *Org. Biomol. Chem.*, 2005, **3**, 1612.
- 3 (a) R. Haynes and S. Vonwiller, *Acc. Chem. Res.*, 1997, **30**, 73; (b) A. Robert and B. Meunier, *Chem. Soc. Rev.*, 1998, **27**, 273; (c) C. Jefford, S. Kohmoto, D. Jaggi, G. Timari, J.-C. Rossier, M. Rudaz, O. Barbuzzi, D. Gérard, V. Berger, P. Kamalaprija, J. Mareda, G. Bernardinelli, I. Manzanares, C. Canfield, S. Fleck, B. Robinson and W. Peters, *Helv. Chim. Acta*, 1995, **78**, 647; (d) W. Hofeinz, H. Burgin, E. Gocke, R. Jacquet, R. Masciadri, S. Schmid, H. Stohler and H. Urwyler, *Trop. Med. Parasitol.*, 1994, **45**, 261; (e) O. Dechy-Cabaret, F. Benoit-Vical, A. Robert and B. Meunier, *ChemBioChem.*, 2000, **4**, 283.
- 4 M. Gavrilan, C. André-Barrès, M. Baltas, T. Tzedakis and L. Gorrichon, *Tetrahedron Lett.*, 2001, **42**, 2465–2468.
- 5 (a) F. Najjar, F. Fréville, F. Desmoulin, L. Gorrichon, M. Baltas, H. Gornitzka, T. Tzedakis and C. André-Barrès, *Tetrahedron Lett.*, 2004, **45**, 6919; (b) C. André-Barrès, F. Najjar, A. L. Bottalla, S. Massou, C. Zedde, M. Baltas and L. Gorrichon, *J. Org. Chem.*, 2005, **70**, 6921; (c) C. Lacaze-Dufaure, F. Najjar and C. André-Barrès, *THEOCHEM*, 2007, **803**, 17.
- 6 (a) L. Sy and G. Brown, *Tetrahedron*, 2002, **58**, 897; (b) R. Schobert, R. Stehle and H. Milhous, *J. Org. Chem.*, 2003, **68**, 9827; (c) C. Bäcktorp, J. Tobias, Johnson Wass, I. Panas, M. Sköld, A. Börje and G. Nyman, *J. Phys. Chem. A*, 2006, **110**, 12204; (d) C. Bowes, D. Montecalvo and F. Sondheimer, *Tetrahedron Lett.*, 1973, **14**, 3181; (e) D. Barton, R. Haynes, G. Leclerc, P. Magnus and I. Menzies, *J. Chem. Soc., Perkin Trans. 1*, 1975, 2055; (f) M. Laguerre, J. Dunogues and R. Calas, *J. Chem. Res.*, 1978, 295; (g) A. Krebs, H. Schmalstieg, O. Jarchow and K.-H. Klaska, *Tetrahedron Lett.*, 1980, **21**, 3171.
- 7 F. Najjar, C. André-Barrès, R. Lauricella, L. Gorrichon and B. Tuccio, *Tetrahedron Lett.*, 2005, **46**, 2117.
- 8 (a) B. Tuccio, R. Lauricella and L. Charles, *Int. J. Mass Spectrom.*, 2006, **252**, 47; (b) I. El Hassan, L. Charles, R. Lauricella and B. Tuccio, *New J. Chem.*, 2008, **32**, 680; (c) M. Triquigneaux, B. Tuccio, R. Lauricella and L. Charles, *J. Am. Soc. Mass Spectrom.*, 2009, **20**, 2013.
- 9 V. Roubaud, H. Dozol, C. Rizzi, R. Lauricella, J. C. Bouteiller and B. Tuccio, *J. Chem. Soc., Perkin Trans. 2*, 2002, 958.
- 10 D. R. Duling, *J. Magn. Reson., Ser. B*, 1994, **104**, 105.
- 11 L. Charles, *Rapid Commun. Mass Spectrom.*, 2008, **22**, 151.
- 12 P. Tordo, *Electron Paramagn. Reson.*, 1998, **16**, 116, and references therein.
- 13 G. Buettner, *Free Radical Biol. Med.*, 1987, **3**, 259, and references therein.
- 14 (a) B. Tuccio, A. Zeghdaoui, J. P. Finet, V. Cerri and P. Tordo, *Res. Chem. Intermed.*, 1996, **22**, 393; (b) C. Rizzi, S. Marque, F. Belin, J. C. Bouteiller, R. Lauricella, B. Tuccio, V. Cerri and P. Tordo, *J. Chem. Soc., Perkin Trans. 2*, 1997, 2513.
- 15 R. Lauricella, A. Allouch, V. Roubaud, J. C. Bouteiller and B. Tuccio, *Org. Biomol. Chem.*, 2004, **2**, 1304.
- 16 A. Rockenbauer, L. Korecz and K. Hideg, *J. Chem. Soc., Perkin Trans. 2*, 1993, 2149.
- 17 V. Bernat, N. Saffon, M. Maynadier, H. Vial and C. André-Barrès, *Tetrahedron*, 2009, **65**, 7372–7379.
- 18 F. W. McLafferty, *Org. Mass Spectrom.*, 1980, **15**, 114.